Memorias del XVI Congreso Latinoamericano de Control Automático, CLCA 2014
Octubre 14-17, 2014. Cancún, Quintana Roo, México

Geometric Model Predictive Control for Three Phase AC Inverters With Linear Loads

Juan M. Alvarez Leiva * **María M. Seron** **
Mónica Romero ***

* *CIFASIS - CONICET, Rosario, Argentina, (e-mail: alvarez@cifasis-conicet.gov.ar).*
** *Centre for Complex Dynamic Systems and Control, The University of Newcastle, Australia, (e-mail: maria.seron@newcastle.edu.au)*
*** *CIFASIS - CONICET and Departamento de Electrónica, FCEIA, National University of Rosario, Argentina, (e-mail: mromero@cifasis-conicet.gov.ar).*

Abstract: In the present work, a study of the geometrical properties of a model predictive control (MPC) strategy for Three-Phase Inverters with a linear load is presented. The studied technique is combined with Space Vector Modulation (SVM) to reduce the harmonic content of the generated signals. The analysis concludes with the development of a control algorithm which exploits the observed geometrical properties in order to achieve a computationally efficient implementation of the MPC-SVM control. The proposed controller is tested in simulation, on a three-phase inverter with an LCL filter.

Keywords: Predictive control, Inverters, Geometric MPC, Space Vector Modulation.

1. INTRODUCTION

In recent days, power electronics has become one of the most studied fields of application of advanced control techniques, due to the increasing need for such devices in a wide range of systems. For example, the integration of renewable energy resources into electric distribution networks relies on power electronics devices working as conditioning interfaces, to cope with the variability of the resource and provide a proper output voltage. Other examples include electrical drives, such as induction motors, which utilize power electronics devices to synthesize the control actions provided by a controller.

Traditionally, controllers have been designed and implemented without considering the commutation of the inverter switches. The control actions are passed as a reference to the inverter, which performs a Pulse Width Modulation (PWM) strategy to synthesize a signal whose first order harmonic's amplitude and frequency equal the given reference values. In an effort to include the modulation techniques into the control algorithms, Model Predictive Control (MPC) is currently being studied. In such algorithms, the control actions are chosen in order to minimize a cost function that quantifies the system's performance along a prediction of its response. The advantage of these methods is that the commutation can be easily introduced by considering that the control actions can only be one of the finite states provided by the inverter. This is sometimes called Finite-States MPC (FS-MPC). Some works in which this kind of techniques are implemented for the control of several power electronics devices are Romero et al. (2011), Rodriguez et al. (2007) and Lezana et al. (2009).

In previous work (see Alvarez Leiva et al. (2013) and Romero et al. (2011)), we have made use of MPC techniques with the addition of Space Vector Modulation (SVM), a commonly used PWM method. The result is obtained by subdividing the sampling period in subintervals. With this discretization, sequences of the inverter states are proposed as the available control actions. The sequences are defined so as to follow the SVM technique. The inclusion of SVM is done to achieve constant switching frequency, resulting in a cleaner harmonic spectrum for low frequencies (as shown in Holmes (1995)). In the present article, this MPC-SVM algorithm is further studied. Some geometrical characteristics of the cost function are analyzed and exploited, obtaining a more computationally efficient method to calculate the optimal sequence, thus called Geometric MPC. The aforementioned geometrical properties are not only present in inverters intended for electrical distribution, hence the development of this technique is aimed at a general linear load. However, in the example we apply the developed technique on a typical circuit used in distributed generation systems such as a Three-Phase Voltage Source Inverter with an LC filter and a coupling inductance, so as to highlight its advantages in such an important field of application.

2. PROBLEM DESCRIPTION

The system under study is a three-phase voltage source inverter with a linear load, whose structure is depicted in Fig. 1. The inverter converts DC power from a DC bus, denoted as V_{DC}, into AC power required by the load.

The control objective is to regulate a three phase AC voltage at some node within the load, with frequency and amplitude as requested by two reference inputs, V_{ref} and ω_{ref} respectively. For example, this regulated voltage may be, in the case of a voltage source inverter with an LC filter, the voltage on the filter capacitor.

The proposed controller is synthesized using MPC combined with SVM. For the control law derivation it is necessary to have a dynamic model of the system composed by the inverter and the linear load. For the load we consider a state space model with the following structure:

$$\dot{x} = Ax + Bu + Ed \qquad (1)$$
$$y = Cx$$

where $x \in \mathbb{R}^n$ is the state vector, d a disturbance vector and u the input vector, which in this case is formed by v_a and v_b (the components of the inverter voltage in the 'ab' reference frame). A, B and E are some matrices defining the dynamics of the load. y is the output vector, which in this case is the voltage we want to control.

The studied inverter (Fig. 1) provides 8 voltage vectors, six of which are active vectors ($V_1 \dots V_6$) and two null vectors ($V_0 = V_7 = 0$), depending on the state of the switches S_1, S_2 and S_3 (each of them corresponding to phases R, S and T respectively), see Fig. 2. Each voltage vector corresponds to a specific voltage value at the output of the inverter.

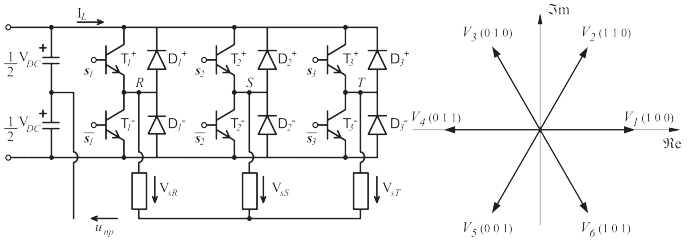

Fig. 1. Inverter's schematic circuit. Fig. 2. Voltage Vectors.

2.1 Space Vector Modulation - SVM

The inverter switches are generally driven using a Pulse Width Modulation (PWM) technique so as to provide the desired output voltage. Some of the most used PWM methods are carrier-based, among which Suboscillation and Space Vector Modulation are highly studied. These methods provide subcycles of constant duration, defining subcycle as the time elapsed between two successive changes in the voltage polarity of any leg of the inverter. In carrier-based methods, the subcycle has a duration of $T_s/2$, where $f_s = 1/T_s$ is the carrier frequency. The benefit of subcycles of constant duration is that they provide a desirable harmonic spectrum of the generated signal, as shown in Holmes (1995).

In SVM, the generated switched three-phase voltage waveform is calculated such that the time average of the associated first harmonic equals a reference signal $u^*(t)$. To achieve this, $u^*(t)$ is sampled at a fix rate of f_s and is used to solve the following equations for t_x and t_y:

$$2f_s(t_x V_x + t_y V_y + t_0 V_{0,7}) = u^*(t_s),\ t_0 = \frac{1}{2f_s} - t_x - t_y \qquad (2)$$

In the equations above, V_x and V_y are two active vectors, adjacent in the 'ab' frame to the reference vector $u^*(t_s)$; and $V_{0,7}$ is one of the two null vectors. Once t_x and t_y have been calculated, an application sequence must be selected. If, for example, the vectors to be applied are V_1 and V_2, a possible sequence that achieves both constant subcycle and the least number of commutations in the switches is

$$V_0 < t_0/2 > V_1 < t_1 > V_2 < t_2 > V_7 < t_0/2 > \qquad (3)$$
$$V_7 < t_0/2 > V_2 < t_2 > V_1 < t_1 > V_0 < t_0/2 >$$

where the 'on-duration' is indicated in brackets. Fig. 3 shows the column voltages V_{R0}, V_{S0} and V_{T0}, for the sequence shown in (3), for some values of t_0, t_x and t_y. In the following section, a method to apply this concept, combined with MPC is described.

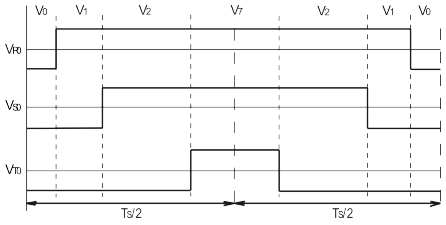

Fig. 3. Example of column voltage under SVM.

3. CONTROL ALGORITHM

3.1 MPC - SVM

MPC is a control technique in which the control action is obtained by solving an open-loop optimization control problem at each sampling interval. A prediction of the response of the system along a given horizon is obtained based on a model of the plant. The control sequence which minimizes a given cost functional represents an open-loop strategy formed by a sequence of control actions to be applied over the prediction horizon. At every sampling interval, the states are measured and used as initial conditions for the prediction, hence turning the control into a closed-loop strategy. Typically, only the first element of the obtained control sequence is applied, and the whole process is repeated in the next sampling instant. This concept is known as Receding-Horizon Control.

In previous articles, see Alvarez Leiva et al. (2013) and Romero et al. (2011), we developed a combined MPC-SVM control strategy. The chosen prediction and control horizon of the MPC controller was 1 sampling interval. This period was divided in subintervals for which control actions are calculated (as described later in this section). The prediction of the system's response is obtained as follows. Let t_k, for $k = 0, 1, \dots$ denote the time instants at the end of the subintervals, and let a subscript k on a variable denote its value at the corresponding instant, *e.g.*, $x_k = x(t_k)$. u_k represents the value of the input vector at the k-th subinterval. Assuming the disturbance d remains constant over a sampling period, the prediction model is then

$$\hat{x}_{k+1} = A_k \hat{x}_k + B_k u_k + E_k d, \qquad (4)$$
$$\hat{y}_k = C\hat{x}_k \qquad (5)$$

where the matrices A_k, B_k and E_k are given by

$$A_k = e^{A(t_k - t_{k-1})},\ B_k = \int_0^{t_k - t_{k-1}} e^{At} B dt,\ E_k = \int_0^{t_k - t_{k-1}} e^{At} E dt \qquad (6)$$

The objective of the controller is to regulate the voltage at some point within the load to have a sinusoidal waveform

with a given amplitude and frequency. Therefore the cost function is defined in terms of the d and q components of the controlled voltage (v_{od} and v_{oq}). In this reference framework, the control objective is achieved if the voltage vector is aligned with one of the axes (namely axis d) of a reference frame which rotates with angular speed equal to the angular frequency reference (ω_{ref}), and its magnitude equals the voltage amplitude reference (V_{ref}). In other words, the control objective is to obtain $v_{od} = V_{ref}$ and $v_{oq} = 0$. To achieve this objective, the cost function for the MPC on-line minimization is defined as

$$J = \sum_{\ell=k}^{\ell=k+N} \left\{ [\hat{v}_{od}(t_\ell) - V_{ref}]^2 + \hat{v}_{oq}(t_\ell)^2 \right\} \qquad (7)$$

To transform the controlled voltage vector into the 'dq' synchronic reference frame, the reference frequency ω_{ref} is integrated to obtain the angle of the reference frame δ, which is used to compute the coordinate transformation shown in (8).

$$\hat{y}_{dq} = \begin{bmatrix} \hat{v}_{od} \\ \hat{v}_{oq} \end{bmatrix} = \underbrace{\begin{bmatrix} \cos\delta(t) & \sin\delta(t) \\ -\sin\delta(t) & \cos\delta(t) \end{bmatrix}}_{\Delta(t)} \hat{y} = \Delta(t)\ \hat{y} \qquad (8)$$

To evaluate the predicted values of the state variables, V_{DC} and the disturbances are measured at each sampling instant and assumed constant over the prediction horizon.

To combine the MPC control with SVM, a parametrization of the control actions was made in a way that they meet the requirements of SVM over a sampling period T_s. This goal is achieved by dividing the sampling period into subintervals during which the applied vector remains constant. Setting some restrictions over which vector can be chosen for each subinterval, and given a number of subintervals to consider, a finite set of possible sequences is obtained. The MPC-SVM controller performs a prediction of the states resulting from the application of each of these sequences, and selects the one that minimizes the cost function (7). Finally, the complete optimizing sequence is applied. It is worth to note that the optimization is done using a sequence of control actions but the actual time horizon is still one sampling period T_s.

The general pattern for the sequences can be seen in Fig. 4.

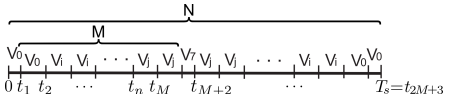

Fig. 4. General pattern for the proposed SVM.

Note that the sequence always starts and finishes with the null vector V_0, and in the middle of the sequence, the null vector V_7 is applied, in order to comply with the SVM requirements. For the rest of the subintervals, the selected subsequences can include null vectors $V_{0,7}$ and two adjacent active vectors: (V_1, V_2), (V_3, V_2), (V_3, V_4), (V_5, V_4), (V_5, V_6) or (V_1, V_6). The subsequence of vectors between V_0 and V_7 in the first half of the pattern is applied in reverse order in the second half of the pattern, between V_7 and the final V_0. More details about the construction of these sequences can be found in Romero et al. (2011) and Holmes (1995).

The control actions resulting from the application of each sequence represent voltage vectors of different magnitudes synthesized to have subcycle of constant duration, *i.e.*, the inverter works at constant frequency.

3.2 Geometric MPC

The objective of this work is to develop a novel implementation of the strategy described in the previous subsection, in which we avoid computing the prediction of the state evolution for every possible sequence. As we show in this section, the method is based on the following principles. We exploit the system's linearity to obtain an explicit expression for the optimal control problem without restraining the control action to be one of the SVM sequences. This leads us to a simple linear state feedback. Then, analyzing geometric characteristics of the associated cost function, we develop a direct and efficient procedure to find which of the available control sequences is the closest to the optimum achieved by the state feedback (closest as with the lowest associated cost). In the remainder of the paper we refer to the first part of the algorithm as finding the 'unconstrained' optimal sequence, even though formally it is still constrained (since the fixed locations of V_0 and V_7 and the symmetric pattern are enforced).

Consider the SVM sequences shown in Fig. 4 with N subintervals. We define vectors X and U as

$$X = \left[\hat{x}^T(t_1)\ \hat{x}^T(t_2)\ \cdots\ \hat{x}^T(t_{2M+3})\right]^T, \quad t_{2M+3} = T_s \qquad (9)$$

$$U = \left[u_0^T\ u_1^T\ \cdots\ u_{N-1}^T\right]^T \qquad (10)$$

$\hat{x}(t_i)$ is the state vector resulting after the application of input u_{i-1}, i.e. the i-th input subinterval of a given sequence. $M = (N-3)/2$ is the number of subintervals between the initial V_0 and the middle V_7 for half a sampling period. Using the prediction equations (4) to (6), we write

$$X = \Lambda x_0 + \Gamma U + \Gamma_d d \qquad (11)$$

for some matrices Λ, Γ and Γ_d. Given the symmetry of the sequences and the repetition of vectors V_0 and V_7, and since the system is linear, we replace the term in (11) that includes the vector U by

$$\Gamma U = \underbrace{\Gamma_0 U_0}_{0} + \Gamma_x U_x \qquad (12)$$

where

$$U_x = \left[u_1^T\ u_2^T\ \cdots\ u_M^T\right]^T \qquad (13)$$

$$U_0 = \left[V_0^T\ V_7^T\ V_0^T\right]^T = 0 \qquad (14)$$

and (11) is rewritten as

$$X = \Lambda x_0 + \Gamma_x U_x + \underbrace{\Gamma_d d}_{U_d}. \qquad (15)$$

Appendix A presents the structure of matrices Λ, Γ_0 and Γ_x.

The output sequence Y_{dq} contains the sequence of controlled voltages obtained by applying input U, transformed into the 'dq' reference frame and is defined as

$$Y_{dq} = \mathbb{C} X \qquad (16)$$

where

$$\mathbb{C} = diag\left(\Delta_1 C, \Delta_2 C, \cdots, \Delta_{2M+3} C\right) \qquad (17)$$

with $\Delta_i = \Delta(t_i)$, see (8).

Using these definitions, the cost function can be written as

$$J = [Y_{dq} - Y_{ref}]^T [Y_{dq} - Y_{ref}] \tag{18}$$

Where

$$Y_{ref} = [\overbrace{\begin{bmatrix} V_{ref}^T & 0 \end{bmatrix} \cdots \begin{bmatrix} V_{ref}^T & 0 \end{bmatrix}}^{(2M+3) \text{ times}}]^T \tag{19}$$

Substituting (15) into (18) we arrive to

$$J = U_x^T H U_x + 2U_x^T \Gamma_x^T \mathbb{C}^T \mathbb{C}[\Lambda x_0 + U_d] - 2U_x^T \Gamma_x^T \mathbb{C}^T Y_{ref} + R \tag{20}$$

where $H = \Gamma_x^T \mathbb{C}^T \mathbb{C} \Gamma_x$ and R is a constant term.

In order to obtain the sequence U_x^{opt} that minimizes the functional J, we compute the derivative of J with respect of U_x, equate to zero, and then solve for U_x, yielding

$$U_x^{opt} = -H^{-1} \underbrace{\Gamma_x^T \mathbb{C}^T [\mathbb{C}\Lambda x_0 + \mathbb{C}U_d - Y_{ref}]}_{f}$$

$$U_x^{opt} = -H^{-1} f(x_0, d, V_{ref}, \omega_{ref}, t) \tag{21}$$

While U_x^{opt} represents the optimal *unconstrained* sequence that minimizes the functional J, it does not necessarily belong to the set of possible sequences obtained by the parametrization described in Section 3.1. We still have to find out which of these sequences has the lowest associated cost. In order to solve this, we perform the following change of variables:

$$V_x = H^{\frac{1}{2}} U_x \tag{22}$$

Solving (22) for U_x, and replacing in (20) and (21) we obtain

$$J = V_x^T V_x + 2V_x^T \left(H^{-\frac{1}{2}}\right)^T f + R \tag{23}$$

$$V_x^{opt} = -H^{-\frac{1}{2}} f \tag{24}$$

Equations (23) and (24) show that the level curves of the cost functional J are $(2M)$-spheres, centered at V_x^{opt}, and radius increasing with J. This implies that if we apply the transformation described in (22) to the elements of the set of possible sequences, we can determine which of them minimizes the functional J by finding the one that minimizes the Euclidean distance to V_x^{opt}.

Fig. 5 shows the level curves, for the particular case in which M=1, in the V plane (*i.e.* after the transformation in (22) is applied). The optimal unconstrained control V_x^{opt} is the center of the circles, marked in red, and the optimal MPC-SVM sequence is the closest point, marked in green. The blue crosses are the inverter active vectors in the V plane.

We can summarize the control algorithm as follows:

- Off-line calculations:
  - Determine an SVM parametrization and obtain the available control sequences.
  - Obtain a model of the load and calculate matrices Λ, Γ_x and $H^{-\frac{1}{2}}$.
  - Obtain the set of SVM sequences transformed as in (22).
- On-line calculations at every sampling period:
  - Sample the state variables and the disturbance.
  - Calculate V_x^{opt} as shown in (24).
  - Calculate the Euclidean distance from every sequence to V_x^{opt}, and apply the one with the lowest value.

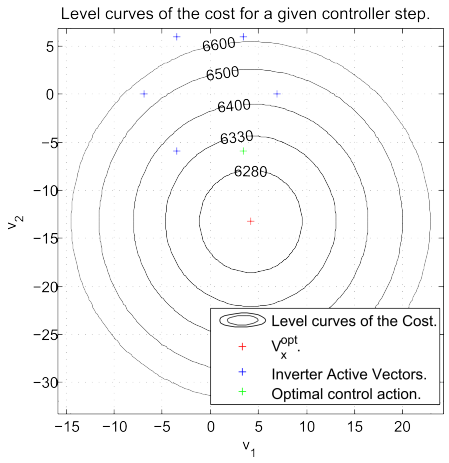

Fig. 5. Geometric interpretation of MPC-SVM

The main advantage of this method is that it divides the problem in two parts, which can be easily solved with a low computational cost. First, a simple linear state feedback is computed (Equation (21)), which gives the optimal unconstrained control action, and then a simple distance calculation is used to find the closest sequence. In other words, given the linear structure of the load, it was shown that finding the optimal sequence can be easily made by (i) solving the optimization problem as if the control action was unconstrained, which leads to a simple and computationally cheap control algorithm (linear state feedback); and (ii) selecting which of the available sequences has the lowest associated cost, which is as simple as calculating an Euclidean distance. This can be applied to any linear load, regardless of its dimensions or structure.

4. APPLICATION EXAMPLE

This section presents an application example consisting of a voltage source inverter with an LCL filter and a linear load. Such a device is commonly found in converters used to interface a distributed power source with a microgrid. The structure of the test plant is depicted in Fig. 6. As the system is intended for AC distributed generation, the LCL filter is needed to damp the high order harmonics introduced by the inverter in order to comply with power quality standards (*e.g.* IEEE1547, see IEEE (2003)).

The proposed controller aims at regulating the voltage of the filter's capacitor. The capacitor voltage (v_o) is controlled, instead of v_b, because this imposes less restrictions to the load. For example if two or more of these devices are connected to the same AC-bus, controlling v_b would lead to a conflict between the controllers acting on the same variable. The parameters of the coupling inductor (L_c and R_c) have to be designed in such a way that the voltage drop is negligible. On the other hand, a supervisory control may be active in order to calculate the references (V_{ref} and ω_{ref}) for the different power sources in the system so as to keep v_b under operational margins.

As we can see in Fig. 6 the filter parameters are: the filter inductance L_f, its loss resistance R_f, the filter capacitor C_f, the coupling inductance L_c and its loss resistance R_c.

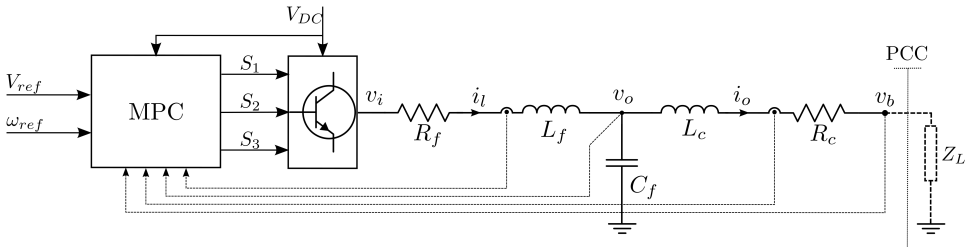

Fig. 6. Schematic of the test system.

A state space model of the filter is derived and the obtained structure for the elements in (1) is shown in (25) to (27).The state variables v_{oa}, v_{ob} represent the 'ab' components of the capacitor voltage, i_{la}, i_{lb} the filter inductance currents and i_{oa}, i_{ob} the coupling inductance currents. The input variables of the filter v_{ia} and v_{ib} are the inverter output voltage components. Finally, v_{ba} and v_{bb} are the 'ab' components of the voltage at the PCC; as this voltage depends on the dynamics of the load we consider it as a disturbance to the model.

$$x = [i_{la}\ i_{lb}\ v_{oa}\ v_{ob}\ i_{oa}\ i_{ob}]^T \tag{25}$$

$$u = [v_{ia}\ v_{ib}]^T\ \ d = [v_{ba}\ v_{bb}]^T\ \ y = [v_{oa}\ v_{ob}]^T \tag{26}$$

$$A = \begin{bmatrix} -\frac{R_f}{L_f} I_{2\times2} & -\frac{1}{L_f} I_{2\times2} & 0_{2\times2} \\ \frac{1}{C_f} I_{2\times2} & 0_{2\times2} & -\frac{1}{C_f} I_{2\times2} \\ 0_{2\times2} & \frac{1}{L_c} I_{2\times2} & -\frac{R_c}{L_c} I_{2\times2} \end{bmatrix} \quad B = \begin{bmatrix} \frac{1}{L_f} I_{2\times2} \\ 0_{2\times2} \\ 0_{2\times2} \end{bmatrix} \tag{27}$$

$$E = \begin{bmatrix} 0_{2\times2} & 0_{2\times2} & -\frac{1}{L_c} I_{2\times2} \end{bmatrix}^T \quad C = \begin{bmatrix} 0_{2\times2} & I_{2\times2} & 0_{2\times2} \end{bmatrix}$$

Table 1. Test System Parameters.

Param.	Value	Param.	Value	Param.	Value	Param.	Value
Inverter Parameters							
R_f	0.15 Ω	L_f	5 mH	C_f	65 μF	f_s	10 KHz
R_c	0.05 Ω	L_c	0.53 mH	V_{DC}	540 V		
Load Parameters				References			
R_{load}	25 Ω	L_{load}	1 mH	V_{ref}	240 V	f_{ref}	50 Hz

All the results shown in this section were obtained in simulation. A model of the system in Fig. 6 was implemented in Matlab/Simulink, and as a load Z_L we considered a linear RL impedance. For the controller, the sequences were divided into 5 subintervals, leading to 91 different sequences from which to choose the one that minimizes the cost function. The simulation parameters are listed in Table 1, where f_s is the sampling frequency. Fig. 7 shows the steady state phase voltages at the filter's capacitor.

In the remainder of this section we analyze both the dynamic performance of the controller, and the improvement in the calculation time, given by the geometric controller.

4.1 Controller Performance

To obtain a quantity representing the performance of the inverter, we calculate the Total Harmonic Distortion (THD) of the output voltage as

$$\%THD = 100\left(H_2^2 + H_3^2 + H_4^2 + \cdots + H_\infty^2\right) / \left(H_1^2\right) \tag{28}$$

where H_1 is the RMS value of the fundamental harmonic, and H_n is the RMS values of the n-th harmonic. The value obtained for the steady state phase voltages of the inverter shown in Fig. 7 is $THD = 0.44\%$. This THD value shows an improvement of the MPC-SVM method over a classic control scheme characterized by nested PI loops with SVM modulation proposed, for example, in Huang et al. (2008) which, using the same parameters of Table 1, presents a $THD = 1.33\%$. Fig. 8 compares the output voltage (v_{od} and v_{oq}) of the proposed controller (MPC-SVM) and the nested PIs structure. It can be seen that for the same circuit parameters and inverter frequency the proposed technique shows a sensibly lower ripple.

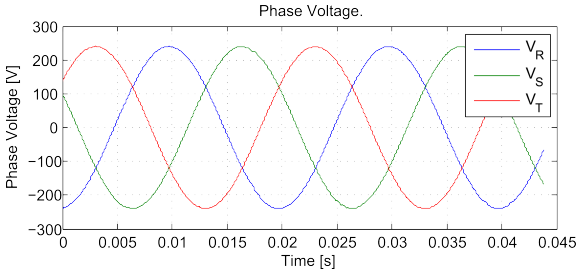

Fig. 7. Steady state phase voltages of the inverter.

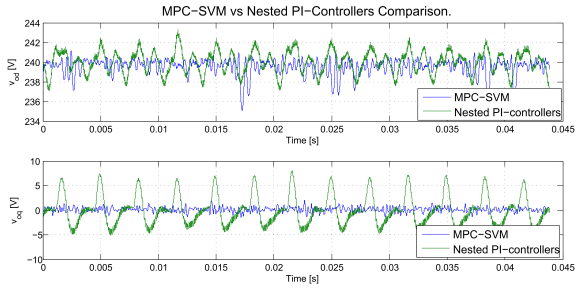

Fig. 8. Output voltage components in steady state, using different controllers.

4.2 Calculation Improvement

In order to analyze the improvement of the computational effort introduced by the geometric implementation, we calculated at every sampling instant both the geometric and the implicit MPC algorithms; and we stored the amount of time used by each of these procedures for the same initial conditions. Fig. 9 shows the execution time of each of the routines for 1000 sampling periods. It is worth mentioning that, as expected, the control actions calculated by both implementations were the same.

We can observe that the reduction in the computational cost between the geometric and the implicit versions of the control algorithm is about 80%. The main cause of this improvement is that it is not required to perform on-line simulations of the system response for every possible sequence. Instead, the calculation of matrices $H^{\frac{1}{2}}$, Γ_x and Λ off-line is required.

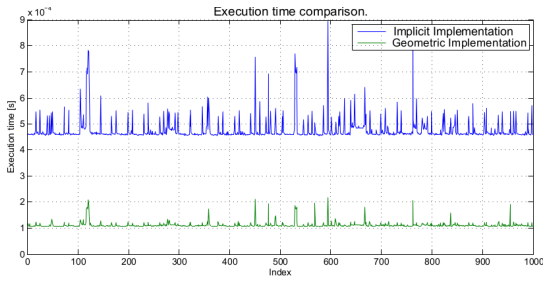

Fig. 9. Execution time comparison between the Geometric and Implicit implementations of the algorithm.

The obtained reduction in the computational effort, versus the implicit implementation of the algorithm provides the possibility of increasing the number of subintervals in a sequence. This would lead to a thinner SVM discretization, thus increasing the available control actions (resulting in the possibility to find sequences closer to the unconstrained optimal). Note that this improvement in the discretization does not imply an increment in the inverter frequency as the SVM technique is applied in the construction of the sequences.

We are currently studying a modification to the presented method to further reduce the computational load. The objective is to reduce the number of sequences in the feasible set where the sequence closest in distance to the unconstrained optimum is selected from. To achieve this, we suggest to calculate the average vector $\mathbf{u}^{opt}$ equivalent to the application of the unconstrained optimal sequence U_x^{opt} over a sampling period, that is, if u_i^{opt} are the entries of U_x^{opt}, then (with T_i as defined in Appendix A),

$$\mathbf{u}^{opt} = 2\left(\sum_{i=1}^{M} T_i u_i^{opt}\right)/T_s = 2T_i\left(\sum_{i=1}^{M} u_i^{opt}\right)/T_s.$$

The above vector can be plotted in the (a, b) plane of Fig. 2 to find in which sextant it lies. Then, we can look for the closest available sequence only among those which are synthesized using the two adjacent vectors that limit the found sextant (and in consequence, result in average vectors in the same sextant). With the discretization used in this example, this means calculating 15 distances instead of 91. Though we have not implemented this modification yet, we are confident that the reduction in the processing time will be sensible. We are currently investigating the degree of suboptimality (if any) of this simplified solution.

5. CONCLUSION

A computationally efficient implementation of MPC-SVM control was proposed for three-phase inverters with a linear load. The technique exploits geometric properties of the cost function in order to reduce the calculation's complexity. The obtained implementation avoids the simulation of the system at every sampling instant and for every possible control sequence by using the associated optimal linear state feedback controller. Then the selection of the sequence with the lowest associated cost is done by finding the one with the minimum Euclidean distance to the output of the state feedback.

The simulation results show an important reduction in the computational cost of the algorithm, versus the former implicit implementation.

REFERENCES

Alvarez Leiva, J.M., Romero, M., and Seron, M. (2013). MPC control for three-phase inverter in stand alone operation. In *RPIC 2013 - XV Reunión de Trabajo en Procesamiento de la Información y Control*.

Holmes, D. (1995). The significance of zero space vector placement for carrier based pwm schemes. In *Industry Applications Conference, 1995. Thirtieth IAS Annual Meeting, IAS '95., Conference Record of the 1995 IEEE*, volume 3, 2451–2458 vol.3. doi: 10.1109/IAS.1995.530615.

Huang, S., Kong, L., Wei, T., and Zhang, G. (2008). Comparative analysis of PI decoupling control strategies with or without feed-forward in SRF for three-phase power supply. In *International Conference on Electrical Machines and Systems, 2008. ICEMS 2008*, 2372–2377.

IEEE (2003). IEEE standard for interconnecting distributed resources with electric power systems. *IEEE Std 1547-2003*, 0_1–16. doi: 10.1109/IEEESTD.2003.94285.

Lezana, P., Aguilera, R., and Quevedo, D. (2009). Model predictive control of an asymmetric flying capacitor converter. *IEEE Transactions on Industrial Electronics*, 56(6), 1839–1846. doi:10.1109/TIE.2008.2007545.

Rodriguez, J., Pontt, J., Silva, C., Correa, P., Lezana, P., Cortes, P., and Ammann, U. (2007). Predictive current control of a voltage source inverter. *IEEE Transactions on Industrial Electronics*, 54(1), 495–503. doi:10.1109/TIE.2006.888802.

Romero, M., Seron, M., and Goodwin, G. (2011). A combined model predictive control/space vector modulation (MPC-SVM) strategy for direct torque and flux control of induction motors. In *IECON 2011 - 37th Annual Conference of the IEEE Industrial Electronics Society*, 1674–1679. doi:10.1109/IECON.2011.6119558.

Appendix A. MATRIX DEFINITIONS

In the following definitions, T_0, T_7 and T_i are the duration of the subintervals in which V_0, V_7 and the remaining vectors in the sequence are applied, respectively. The sampling time then satisfies: $T_s = 2T_0 + 2MT_i + T_7$.

$$A_0{=}e^{AT_0},\ A_s{=}e^{AT_i},\ A_7{=}e^{AT_7},\ B_s{=}\int_0^{T_i} e^{At}Bdt, \tag{A.1}$$
$$E_0{=}\int_0^{T_0} e^{At}Edt,\ E_s{=}\int_0^{T_i} e^{At}Edt,\ E_7{=}\int_0^{T_7} e^{At}Edt$$

$$\Lambda{=}\begin{bmatrix}\lambda_1\\ \lambda_2\\ \vdots\\ \lambda_N\end{bmatrix},\ \Gamma_x{=}\begin{bmatrix}\gamma_{1,1} & \gamma_{1,2} & \cdots & \gamma_{1,M}\\ \gamma_{2,1} & \gamma_{2,2} & & \gamma_{2,M}\\ \vdots & & \ddots & \vdots\\ \gamma_{N,1} & & \cdots & \gamma_{N,M}\end{bmatrix},\ \Gamma_d{=}\begin{bmatrix}\gamma_{d1}\\ \gamma_{d2}\\ \vdots\\ \gamma_{dN}\end{bmatrix} \tag{A.2}$$

$$\lambda_i{=}\begin{cases}A_s^{i-1}A_0 & \text{if } i{\le}M{+}1\\ A_s^{i-M-2}A_7A_s^MA_0 & \text{if } M{+}1{<}i{<}2M{+}3\\ A_0A_s^MA_7A_s^MA_0 & \text{if } i{=}2M{+}3\end{cases} \tag{A.3}$$

$$\gamma_{i,j}{=}\begin{cases}O^{n\times 2} & \text{if } i{\le}j\\ A_s^{i-j-1}B_s & \text{if } j{<}i{\le}M{+}1\\ A_7A_s^{M-j}B_s & \text{if } i{=}M{+}2\\ A_s^{i-M-2}A_7A_s^{M-j}B_s{+}A_s^{i+j-2M-3}B_s & \text{if } 2M{+}3{-}j{\le}i{<}2M{+}3\\ A_0A_s^MA_7A_S^{M-j}B_s{+}A_0A_s^{j-1}B_s & \text{if } i{=}2M{+}3\\ A_s^{i-M-2}A_7A_s^{M-j}B_s & \text{Otherwise}\end{cases} \tag{A.4}$$

$$\gamma_{di}{=}\begin{cases}E_0 & \text{if } i{=}1\\ A_s^{i-1}E_0{+}\left(\sum_{l=0}^{i-2}A_s^l\right)E_s & \text{if } 1{<}i{<}M{+}2\\ A_7\left[A_s^ME_0{+}\left(\sum_{l=0}^{M-1}A_s^l\right)E_s\right]{+}E_7 & \text{if } i{=}M{+}2\\ A_s^{i-M-2}\gamma_{d(M+2)}{+}\left(\sum_{l=0}^{i-M-3}A_s^l\right)E_s & \text{if } M{+}2{<}i{<}2M{+}3\\ A_0\left[A_s^M\gamma_{d(M+2)}{+}\left(\sum_{l=0}^{M-1}A_s^l\right)E_s\right]{+}E_0 & \text{if } i{=}2M{+}3\end{cases} \tag{A.5}$$